Engineering 58 (2026) 157–168

Contents lists available at ScienceDirect

Engineering

journal homepage: www.elsevier.com/locate/eng

Research
Biochemical Engineering—Article

Thermostabilizing Functional Proteins with Matrix-Assisted Room-Temperature Drying

Yejiong Yu, Siqi Dai, Johnny Xiangyi Zhou, Wei E. Huang, Zhanfeng Cui *

Department of Engineering Science, University of Oxford, Oxford OX1 3PJ, UK

ARTICLE INFO

Article history:
Received 10 November 2023
Revised 15 September 2024
Accepted 8 August 2025
Available online 9 February 2026

Keywords:
Protein stabilization
Matrix-assisted room temperature drying
Bioproduct drying
Lactate dehydrogenase
Fibroblast growth factor-2
RT-LAMP reagents

ABSTRACT

This study evaluated the efficacy of the proposed matrix-assisted room-temperature (MART) drying as an alternative to freeze-drying for the thermostabilization of functional proteins in a solid state. To achieve this, protective agents were formulated with functional proteins, and the mixture was dried on a biocompatible cellulose fiber matrix. Drying was carried out at room temperature or elevated temperatures (~30 °C), either through dry air circulation (MART-DA drying) or under a vacuum (MART-V drying). The entire drying process did not involve any refrigeration or freezing steps. The results demonstrated the successful thermostabilization of lactate dehydrogenase (LDH), fibroblast growth factor-2 (FGF-2), and functional enzymes in reverse transcription loop-mediated isothermal amplification (RT-LAMP) reagents through the use of MART drying. The functional proteins were immobilized and effectively encapsulated in sugar glass films, preserving the proteins' native structure and functions. The sugar glass films were supported by a low-cost three-dimensional (3D) cellulose fiber matrix. Overall, MART drying offers a simple, fast, low energy-consumption, and cost-effective strategy for drying functional proteins for long-term room-temperature storage.

© 2026 THE AUTHORS. Published by Elsevier LTD on behalf of Chinese Academy of Engineering and Higher Education Press Limited Company. This is an open access article under the CC BY license (http://creativecommons.org/licenses/by/4.0/).

1. Introduction

Due to their inherent instability and susceptibility to degradation, proteins require preservation measures when removed from their native conditions [1–5]. To ensure their efficacy, protein solutions are commonly stored in frozen or solid states for long-term storage. Cryopreservation or low-temperature storage in the frozen state not only retards the degradation process but also prevents microbial growth and foaming during transportation [6–8]. However, the process of freezing can induce stresses resulting from the ice–water interface, solute concentration, and pH shift, which may disturb the native structure of the protein. Therefore, the addition of cryoprotectants is essential to mitigate these stresses and preserve the structural integrity of the proteins [9–14].

The use of a temperature-controlled supply chain, commonly referred to as a "cold chain," is crucial for maintaining optimal temperatures during the low-temperature preservation of protein products and their transportation from manufacturers to customers [15–20]. However, the implementation of such a system comes at a high expense, limiting the coverage of thermolabile protein products, especially in regions that still lack electricity [21,22]. Even in developed countries, temperature regulation during shipping is often inadequate, resulting in a high wastage rate [23,24].

To ease long-term storage and transportation requirements, proteins can be dried or dehydrated with protective agents [25–28]. After water molecules have been removed, the degradation processes are substantially suppressed. The protective agents protect the protein molecules by substituting for the water molecules, and also increase the glass transition temperature, which is the transition temperature between the rigid and soft states of the polymer changes. The higher glass tranistion temperature of the dried product allows for a higher storage temperature [29,30]. Drying processes are commonly done at reduced temperatures to prevent biochemical degradation of the proteins. Freeze-drying, or lyophilization, is a well-established technique for the drying of bioproducts that involves the sublimation of water from a completely frozen sample under a vacuum [31,32]. However, this technique induces both freezing and drying stresses, making it more challenging to design the formulation of protective agents [33–35]. The high capital and operational expenses associated with freeze-drying (as the process is energy intensive and has a long

* Corresponding author.
E-mail address: zhanfeng.cui@eng.ox.ac.uk (Z. Cui).

https://doi.org/10.1016/j.eng.2025.08.045
2095-8099/© 2026 THE AUTHORS. Published by Elsevier LTD on behalf of Chinese Academy of Engineering and Higher Education Press Limited Company.
This is an open access article under the CC BY license (http://creativecommons.org/licenses/by/4.0/).

process duration) increase the final product's cost and limit its applicability [36–38].

We have proposed an alternative approach for drying proteins and other bioproducts called matrix-assisted room-temperature (MART) drying [39]. MART drying uses three-dimensional (3D) porous matrices to load a solution of biological products, supplemented with sugars, and removes water at ambient temperature. MART drying, which is capable of preserving the functionalities of proteins or other products, has the potential to save a substantial amount of energy and drying time in comparison with freeze drying.

The MART drying concept is based on the "sugar film drying" applied for the preservation of biological products. In sugar film drying, a bioproduct solution is mixed with protective agents and transferred into tubes or dripped onto substrates (i.e., a well plate or fiber matrix), followed by overnight room-temperature drying [40–43]. For example, a herpes simplex virus type 2 vaccine and an influenza A vaccine were dried with trehalose and pullulan in Eppendorf tubes using this method. After overnight drying in a biosafety cabinet, their potencies were retained for several weeks at 40 °C, although their effectiveness dropped during the first four weeks of storage [42,44]. Sugar film drying has also been used to stabilize two viral vaccine vectors, the attenuated poxvirus-modified vaccinia virus Ankara (MVA) and E1/E3-deleted human adenovirus type 5 (AdHu5), on a glass fiber matrix. These two vaccine vectors were found to be effective after drying and storage for up to six months at 45 °C [40–43]. However, the use of glass fiber as a matrix is limited by its brittleness. Shattered fragments caused during transportation may enter the human body during administration, leading to allergic reactions [45]. To address this issue, seven other fiber matrices with different properties, such as fiber diameter, porosity, and hydrophilicity, have been evaluated experimentally. However, the outcome for the drying of various vaccines on those fiber matrices did not reach the same level as the glass fiber, only which form capillary bridges among fibers before and after drying. [46].

A mechanism study was carried out to identify the formation of capillary bridges as the key to the success of the MART drying outcome. A numerical simulation was conducted to model the evaporation kinetics of a capillary bridge containing trehalose at different concentrations [47]. The simulation results clearly demonstrated that, on hydrophilic fibers, the capillary bridge took on a shape that was thinnest at the central area and enlarged toward the sides. This shape led to the formation of concentration gradients of trehalose within the bridge during the drying process. These concentration gradients, in turn, generated surface tension gradients, resulting in Marangoni flows that pushed bioproducts toward the central area. Consequently, bioproducts gathered at the central area and were encapsulated with high-concentration protective agents. This encapsulation provided 3D support to the bioproducts, thereby enhancing their stability.

This paper focused on an experimental study to assess the efficacy of MART drying in stabilizing functional proteins, as functional protein drying has significant relevance in various applications, such as biomedical and biopharmaceutical formulation, biotechnology, and the food industry. A biocompatible cellulose fiber matrix was used as the matrix, and four indicative proteins were selected for the experiments. A freeze-sensitive enzyme, lactate dehydrogenase (LDH), was chosen to ensure no freezing stresses were invovled during the drying process [48,49], as well as for its ease of assessment for any functional loss. Then, temperature-sensitive fibroblast growth factor-2 (FGF-2) was also selected for drying. While FGF-2 is commonly used for cell culture and wound healing applications due to its ability to simulate cell proliferation [50–52], its biomedical applications are limited, as it needs to be stored at a low temperature, usually −20 °C. MART drying was employed to enhance its thermostability, and the resulting FGF-2-loaded MART matrix showed potential for direct application to wounds. In addition, a kit for detecting coronavirus disease 2019 (COVID-19) via reverse transcription loop-mediated isothermal amplification (RT-LAMP) was stabilized through MART drying. This kit contains multiple enzymes and substrates that traditionally necessitate storage at low temperatures. However, with MART drying, they can be transported and stored at ambient temperatures, which is a crucial factor for point-of-care testing, especially in areas where cold storage space is limited [53,54].

Two drying protocols, standard MART drying by circulating dry air (MART-DA drying) and MART drying under a vacuum (MART-V drying), were conducted in this study. The effectiveness of MART drying in preserving the bio-functionalities and structural integrity of the functional proteins were investigated, while the influence of operational and formulation variables were assessed.

2. Material and methods

2.1. Materials

Animal-free recombinant human FGF-basic (AF-100-18C) was obtained from PeproTech, UK. Bovine serum albumin (BSA; A9647), *L*-LDH (101278760001), *D*-(+)-trehalose dihydrate (90210), and dextran with relative molecular mass (M_r) approximately 40 000 (31389) were purchased from Sigma-Aldrich, UK. RT-LAMP reagents (E1700) containing WarmStart reverse transcriptase and Bst 2.0 polymerase were obtained from New England Biolabs (NEB, UK). The primers were synthesized by Integrated DNA Technologies (IDT Inc., Belgium). The sequences of primers are listed in Table S1 in Appendix A.

2.2. Fiber matrix preparations

For LDH and FGF-2 stabilization, 20 mg of cellulose fibers were placed in each well of a 48-well plate and compressed into a disc with a thickness of 0.8 mm. The compressed fiber matrices were then carefully taken out of the well by tweezer and placed onto a flat plate. For RT-LAMP reagents stabilization, 5 mg of fibers were compressed into low-profile polymerase chain reaction (PCR) tube strips (Bio-Rad, UK).

2.3. Matrix-assisted room-temperature drying

2.3.1. MART-DA drying

Prior to experimentation, the drying apparatus (Fig. 1) was turned on and left to stabilize for a period of 2 h. The drying apparatus were maintained at 30 °C and 3% relative humidity. The desired functional proteins with excipients were loaded onto the fiber matrices, which were then placed onto the sample station. The matrices were subjected to an 18 h drying process before being transferred to lyophilization vials, which were previous stored in glove box with low relative humidity (< 3%). These vials were then sealed into moisture barrier bags (RS Components Ltd., UK) in a glove box. Finally, the bags were placed into incubators with different temperatures for stability tests.

2.3.2. MART-V drying

Once the fiber matrices were loaded into the designated containers, such as lyophilization vials (Fisher Scientific, UK) or PCR tubes (Thermo Fisher, UK), the formulated proteins were loaded onto the fiber matrix. These containers were then placed into drying bottles that were connected to the manifold of a freeze dryer (Genesis, SP Scientific, USA). Only the vacuum pump of the freeze

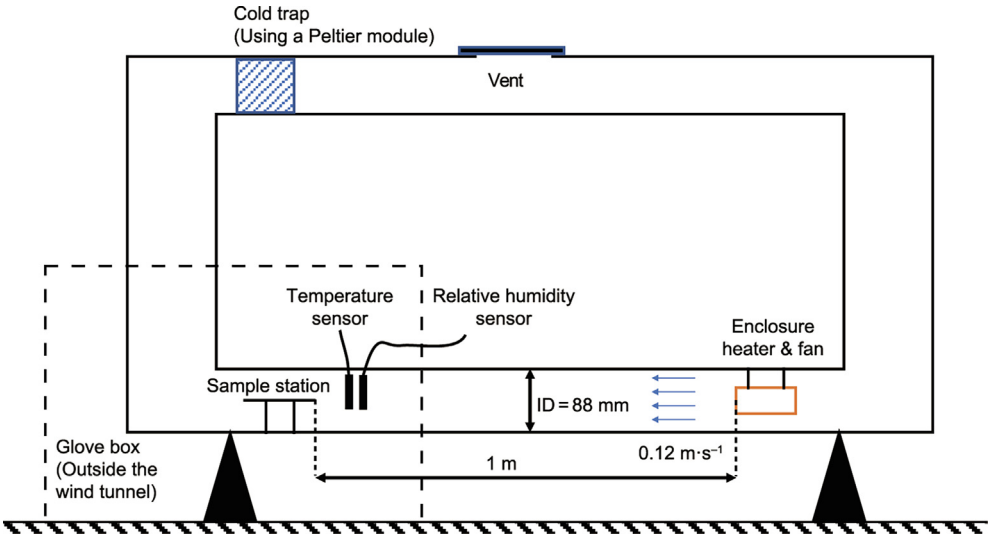


Fig. 1. Schematic diagram of the drying apparatus. Samples were placed on the sample station for MART-DA drying. The circulated air was heated and driven by the enclosure heater and fan (RS Components Ltd.). The temperature of dry air was measured using a temperature sensor and controlled by a proportional–integral–derivative (PID) controller (RS Components Ltd.). The relative humidity of the system was controlled by a cold trap. A Peltier module (RS Components Ltd.) was applied with a heat sink (RS Components Ltd.). Moisture was removed via condensing and freezing on the heat sink.

dryer was switched on for 3 h to remove moisture from the samples. After the drying process was completed, the drying bottles were detached from the freeze dryer and opened inside the glove box, where the relative humidity was kept below 3%. The samples were transferred into moisture-barrier bags and stored in the incubator with different temperatures for stability tests.

2.4. Protein quantification

Each MART-dried matrix was reconstituted by adding 2 mL of deionized water and mixing through pipetting. Protein quantification was carried out using the Quant-iT Protein Assay Kit (Q33210, Thermo Fisher), following the manufacturer's protocol, which included preparing the working buffer by diluting the protein reagent 1:200 into protein measuring buffer. BSA solutions at various concentrations (10 μL each) were mixed with 200 μL of working buffer and used as standards for the measurement. Additionally, 10 μL samples were mixed with 200 μL of working buffer. Furthermore, a solution with the same formulation, except for the addition of LDH, was also dried by MART drying. After reconstitution, protein quantification was conducted in the reconstituted solution as background measurements.

2.5. Determination of LDH activity

After reconstitution by 2 mL of deionized water, the LDH activity assay kit (MAK066) from Sigma Aldrich (UK) was used for LDH activity measurements. For 100 μg LDH measurements, a further 10× dilution was conducted. Then, 2 μL of samples were added to a 96-well plate. For 1 μg LDH measurement, 40 μL of reconstituted samples were added to a 96-well plate. Following the protocol provided by the manufacturer, the sample was mixed with buffer and substrate. After incubating at 37 °C for 2 min, the plate was transferred to a plate reader (SpectraMax i3x, Molecular Devices, UK), which was set to 37 °C as well. The absorption at the wavelength of 480 nm was recorded every 1.5 min. The activity was calculated based on the sample volume added to the well and the slope of the absorbance over time.

2.6. Cultivation of immortalized mesenchymal stem cells

Human bone marrow mesenchymal stem cells transduced with human telomerase reverse transcriptase (MSC-hTERT) were cultured for seven days before the commencement of the experiments. The cells were seeded in tissue culture-treated T-25 flasks (Falcon, UK) and 96-well plates at a cell seeding density of 5000 cm^{-2} with low-glucose Dulbecco's modified Eagle medium (DMEM; Gibco, UK) supplemented with 1% fetal bovine serum (Gibco) and 1% insulin–transferrin–selenium–ethanolamine (ITS-X; Gibco).

MART-V-dried, MART-DA-dried, and −80 °C-stored FGF-2 groups were mixed with the media to prepare the experimental media. Because of the non-sterile drying conditions in the MART-DA- and MART-V-dried groups, the reconstituted experimental media underwent filtration through a 0.22 μm syringe filter before being applied to cells. Control group experimental media were prepared in the same way without FGF-2. A medium change was performed the day after seeding and then every other day to introduce FGF-2 to the cells cultured in 96-well plates.

For the biocompatibility test, the cellulose fiber matrix was carefully added to cultures in T-25 flasks without disturbing the cells on the day after seeding. Control group cells were cultured without the fiber matrix. A medium change was performed every other day.

2.7. MSC-hTERT propagation and fiber matrix biocompatibility test

The proliferation rates of MSC-hTERT cells cultured with the different experimental media were assessed with Cell Counting Kit-8 (CCK-8) purchased from Dojindo, UK. The manufacturer provides a detailed protocol for the assay. In brief, for each well of a 96-well plate, 10 μL of the assay reagent was added to 100 μL of culture medium, followed by incubation at 37 °C for 2 h. During incubation, the assay reagent reacted with the live cells to produce formazan dye, which absorbs light at the wavelength of 450 nm. The plate was then read for light absorbance at 450 nm with a SpectraMax i3x plate reader (Molecular Devices). A standard calibration curve was plotted for optical density against live cell count.

The assay was performed on day 1 (the day after seeding), day 3, day 5, and day 7 to determine the proliferation rates of the different cultures.

2.8. RT-LAMP-lateral flow test (LFT) assay

The primer set (QO117), synthesized by IDT Inc., was designed to target the open-reading frame 1ab (ORF1ab) region of severe acute respiratory syndrome coronavirus 2 (SARS-CoV-2). After being reconstituted by RNase/DNase-free water (10977035, Invitrogen, UK), a 10× labeled primer mix (16 $\mu mol \cdot L^{-1}$ (μM) carboxyfluorescein (FAM)–forward internal primer (FIP) and biotin–backward internal primer (BIP), 2 μM B3 and F3, and 4 μM loop forward (LF) and loop backward (LB)) was prepared.

Loop-mediated isothermal amplification (LAMP) reagents—including 12.5 μL of NEB WarmStart LAMP kit (E1700), 2.5 μL of 10× labeled primer mix, and protective agents—were transferred to 5 mg of fiber matrix, which was previously placed in the PCR tubes. Following the MART-V drying process, the PCR tubes were sealed with caps and placed within moisture-barrier bags.

To evaluate the effectiveness of the MART-V-dried LAMP reagents after one week of storage, full-length synthesized SARS-CoV-2 RNA (Twist Control 2) from Twist Bioscience was added to the positive control, while human genomic DNA (4312660, Thermo Fisher) was added to the negative control. The tubes were placed on ice before the reaction. The reactions were heated at 65 °C for 30 min and at 95 °C for 5 min, denaturing the enzymes, in a CFX OPUS 96 real-time PCR machine (Bio-Rad). After cooling down to room temperature, 5 μL of LAMP product was dripped on the lateral flow strips (Zhongxin Keju Biological Pharmaceutical Co., Ltd., China) and run with 80 μL of phosphate buffer supplied by Zhongxin Keju.

The concentration of Twist Control in the sample was evaluated by means of a quantitative PCR (qPCR) assay on the CFX OPUS 96 real-time PCR machine using the GoTaq Probe one-step RT-qPCR kit (A6121, Promega, UK) with CDC N1 primers (1006770, IDT Inc.). The thermal cycle was set as holding at 45 °C for 15 min and then at 95 °C for 2 min, followed by 45 cycles of 3 s at 95 °C and 30 s at 55 °C. The cycle threshold (CT) values were given by the qPCR machine.

2.9. Microscopic imaging

The dried fiber matrices with formulated proteins were imaged via scanning electron microscopy (SEM). Fiber matrices were mounted onto aluminum mounts with conductive copper tape. After being coated with gold, the fiber matrices were imaged using a Zeiss Sigma 300 field emission gun scanning electron microscope (FEG-SEM; Zeiss, Germany) under vacuum. An acceleration voltage of 2 kV was used.

2.10. Statistical analysis

Statistical differences of the data from the same timepoint but different conditions were analyzed by means of *t*-tests. Differences between groups with various timepoints were analyzed by analysis of variance (ANOVA). *P* values between groups of less than 0.05 were considered a significant difference. The statistical analysis was performed with GraphPad Prism 6.0.

3. Results and discussions

3.1. MART drying of LDH

LDH is naturally vulnerable to freezing, which causes it to lose considerable enzyme activity after one freeze–thaw cycle [55–57], increasing the lyophilization difficulty [58,59]. In this study, LDH was selected as a model protein to investigate the feasibility of MART drying.

3.1.1. Effectiveness of sugars over drying and storage in MART-DA drying

Proteins have the propensity to adsorb on solid surfaces [60,61], which can lead to reduced protein activity. In this study, approximately 7.7 μg of LDH was found to be adsorbed on a 20 mg fiber matrix, as illustrated in Fig. S1 in Appendix A. To minimize the effect of adsorption, a higher LDH amount (100 μg in total) was initially studied. The lower LDH concentration will be discussed in the following sections. Furthermore, it should be noted that the hydrophilicity of the fiber matrix can affect the enzyme activity measurements (Fig. S1). As such, the enzyme activities before drying were measured after adding LDH to the fiber matrix, as the initial enzyme activity.

To mitigate the drying stresses, 100 μg of LDH was formulated with sugars, trehalose, and dextran, which did not affect the enzyme activity (Fig. S2 in Appendix A) and was dried on a low-cost fiber matrix by means of circulated dry air (MART-DA drying). As indicated in Fig. 2(a), the protective function of trehalose exhibited a dose-dependent increase and reached a plateau at 500 $mmol \cdot L^{-1}$ (mM), where it preserved 88% of the initial LDH activity. Beyond this concentration, additional trehalose did not enhance the protective function. The addition of 10% dextran to 500 mM trehalose further enhanced the retained activity to 92.83%, while using dextran alone provided marginal protection (Fig. 2(b)). Dextran has been reported to mitigate the crystallization of sugars during the drying process [62], thereby enhancing the efficacy of functional proteins post-drying. In addition, the glass transition temperature, as measured via differential scanning calorimetry (DSC), showed an increase from 54.81 °C for 500 mM trehalose only to 60.04 °C when combined with 10% dextran (Table 1; Fig. S3 in Appendix A provides detailed DSC figures). The DSC curve of the fiber matrix (Fig. S3(e)) revealed no glass transition or melting phenomena within the temperature range of 0–80 °C.

However, after the MART-dried samples had been stored at 40 °C for one week, the retained activity notably dropped (Fig. 2(c)). Specifically, 75% of the initial activity was retained after storage at 25 °C, while only 56% was retained after storage at 40 °C. This decrease was likely attributed to stress relaxation during storage, as observed from the DSC data (Figs. S3(b) and (c)).

Stress relaxation is a phenomenon that occurs in glassy materials; it involves small conformational changes and the motion of specific chemical groups or short sequences of molecules, a regime with low density and few intermolecular forces [63–68]. This molecular motion can lead to a local increase in material stiffness [69] or recrystallization [70], which can affect the local conformation of proteins and result in denaturation. Previous studies have shown that increasing the concentration of trehalose in the formulation can inhibit stress relaxation and improve the stability of proteins during storage [71–73].

As shown in Fig. 2(d), the extent to which the LDH retained its activity following one week of storage at a temperature of 40 °C was significantly influenced by the concentration of trehalose. A retention rate exceeding 90% of the initial activity was achieved following storage when drying with 1 $mol \cdot L^{-1}$ (M) trehalose and 10% dextran, while no significant improvement was observed when the concentration of trehalose was over 1 M. This particular formulation not only increased the retained activity but also raised the glass transition temperature to above 70 °C, thereby preventing any stress relaxation during storage. The protein quantity was assessed both before and after MART-DA drying, revealing that over 90% of the initial proteins were retained (Table 2).

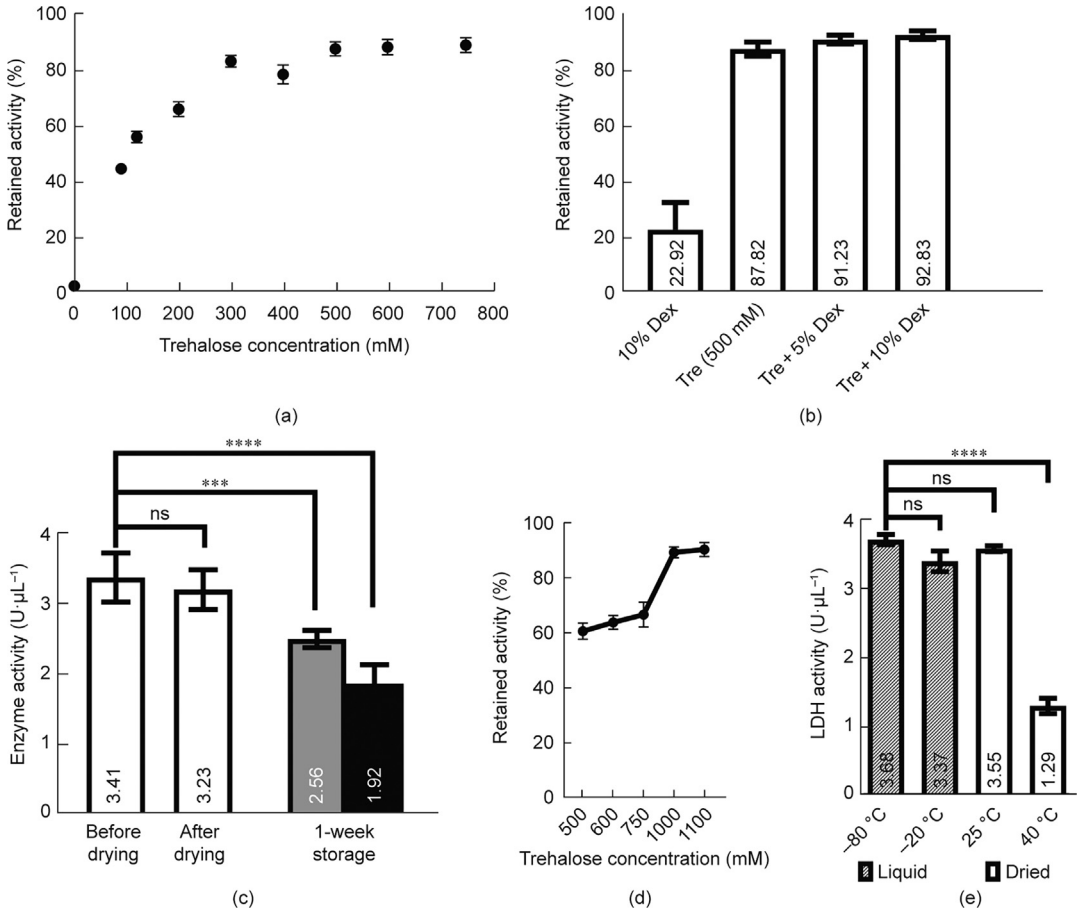


Fig. 2. Preserving LDH with MART drying and stability analysis. (a) Percent retained activities of LDH formulated with different concentrations of trehalose, ranging from 0 to 800 mM. (b) Percent retained activities after drying with different sugar combinations and concentrations (Dex: dextran; Tre: trehalose). (c) Enzyme activities of LDH formulated with 500 mM trehalose with 10% dextran measured before drying, after drying, and after one week of storage at different temperatures (25 °C (grey) and 40 °C (black)). (d) Percent retained activities of MART-DA-dried LDH formulated with elevated trehalose concentration with 10% dextran, measured after one week of storage at 40 °C. (e) LDH activities measured after six months of storage under different storage conditions. Results are presented as mean ± standard error of the mean (sem); $n = 3$; ns: no significant difference; $^{*}P < 0.05$, $^{**}P < 0.01$, $^{***}P < 0.001$, and $^{****}P < 0.0001$.

Table 1
Glass transition temperatures (T_g) of MART-DA-dried LDH with different formulation and storage conditions.

Formulation	Storage conditions	T_g (°C)
500 mM Tre	After drying	54.81
500 mM Tre + 10% Dex	After drying	60.04
500 mM Tre + 10% Dex	After drying and storage at 25 °C for 1 week	58.27
	After drying and storage at 40 °C for 1 week	64.38
1000 mM Tre + 10% Dex	After drying and storage at 25 °C for 1 week	72.33
	After drying and storage at 40 °C for 1 week	81.64

Table 2
Protein quantification before and after MART drying.

Sample	Protein concentration (μg BSA equivalent)	Recovery percentage (%)
Fresh LDH	109.28 ± 2.53	–
MART-DA-dried LDH	101.95 ± 1.59	93.3
MART-V-dried LDH	98.38 ± 0.97	90.0

The glass transition temperature of the product stored at 40 °C was observed to always be slightly higher than that stored at 25 °C (Table 1); this could be caused by the moisture absorbents, which were placed with the samples together in the moisture-barrier bags. More desiccation occurred at a higher temperature, leading to lower moisture content and a higher glass transition temperature after storage.

Optimization of the drying parameters was crucial to ensure the stability of the LDH formulation during the drying process. Various factors including the drying temperature, relative humidity, fiber matrix thickness, and drying time were taken into consideration, and the ideal conditions were established based on the findings presented in Fig. S4 in Appendix A. The LDH formulation, composed of 1 M trehalose and 10% dextran, was subjected to drying on an 8 mm-thick fiber matrix at 30 °C with a relative humidity of 3% over a duration of 18 h. This process effectively preserved the bio-functionalities of LDH after drying. The dried samples were then subjected to long-term stability testing at temperatures of 25 and 40 °C, while control groups were stored at −20 and −80 °C for comparison purposes.

The LDH samples dried using the MART-DA technique exhibited remarkable retained activities, even after six months of storage at a temperature of 25 °C, achieving the same level as those that had been cryopreserved (Fig. 2(e)). Although the two control groups (−20 and −80 °C) showed no significant difference in retained activity, it should be noted that the high variation observed in the −20 °C storage group might be attributed to solute precipitation, as illustrated in Fig. S5 in Appendix A. It was evident

that the enzyme activities declined considerably when the samples were stored at 40 °C, as protein hydrolysis and aggregation cannot be entirely prevented even in a solid state [31,74,75]. The relatively high LDH concentration and elevated temperature may have contributed to the aggregation. Overall, the results of this study demonstrate that the MART-DA technique has great potential in preserving the activity of LDH at ambient temperatures.

3.1.2. Protein adsorption on the fiber matrix

To explore the feasibility of using the MART drying technique, a reduced amount (1 μg in total) of LDH was dried on the same cellulose fiber matrix. However, due to solid-surface adsorption, the LDH was adsorbed on the well plate during the drying process, leading to a complete loss of activity (group 1 in Fig. 3(a)). Although the addition of sugars slightly reduced the adsorption on the well plate (group 2), it did not provide a significant improvement when combined with the fiber matrix (group 4).

The adsorption of LDH onto the well plate was effectively reduced by its co-mixing with BSA (control group, group 3). However, when the protein solution was mixed with BSA prior to being applied to the fiber matrix (group 5), it exhibited lower activity compared with the control group (group 3). The introduction of the desired proteins onto the fiber matrix precoated with BSA significantly decreased adsorption (group 6), yielding results comparable to those observed in the control group (group 3).

Coating with BSA is an inexpensive and readily available method of antifouling application [76–78], and BSA's non-reactive properties make it widely applicable as a blocker for immunohistochemistry [79,80] and other biological assays [81,82]. Following the application of BSA coating, BSA's inherent zwitterionic property and negative surface charge contribute to the prevention of biomolecular adhesion, mitigating non-specific binding and maintaining the activities of the proteins [78,83]. It should be noted that the activity of LDH in this experiment was relatively lower than that in the previous experiments, which could be due to the aging of the enzyme or the frequent opening of the LDH container in a non-sterile environment. While MART-DA drying provides a higher mass transfer rate and evaporation rate due to its expanded surface contact area and elevated drying temperature in comparison with lyophilization, the complete drying process still required an 18 h duration.

3.1.3. MART-V drying of LDH

To shorten the drying time, the feasibility of using MART-V drying was explored in order to stabilize the functional proteins by drying under a vaccum. It was found that a 3 h MART-V drying process achieved the same moisture content in the dried matrix as the 18 h MART-DA drying process (Fig. S6 in Appendix A).

In terms of LDH stabilization, MART-V drying was able to retain approximately 91.37% of the initial LDH activity, which was comparable to the retention achieved by MART-DA drying (92.14%). After one week of storage, the activity of the MART-V-dried LDH was retained at 85.64% for 25 °C storage and 81.04% for 40 °C storage, respectively, and there was no statistical difference compared with the MART-DA-dried LDH.

The protein quantification carried out before and after the MART drying of 100 μg of LDH also revealed no significant difference between MART-DA drying and MART-V drying (Table 2).

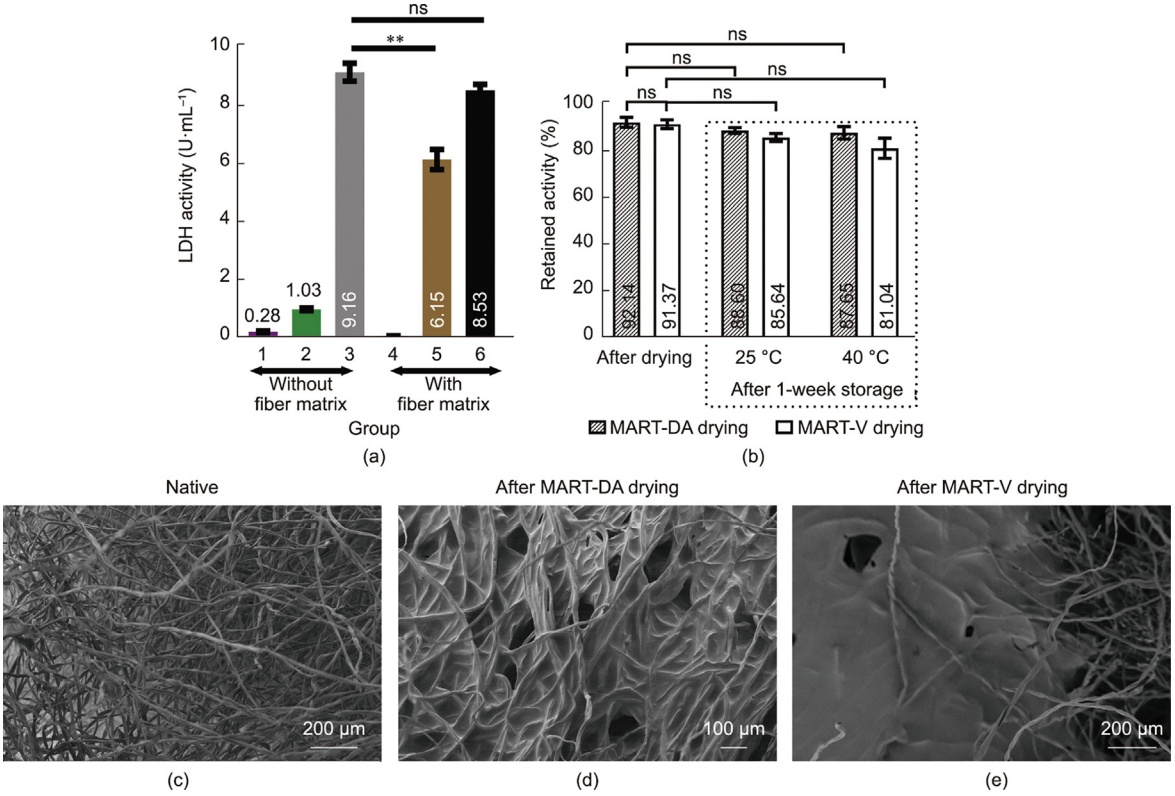


Fig. 3. Nonspecific binding mitigation with BSA coating and feasibility test with MART drying. (a) LDH activity with different excipients without and with the fiber matrix (groups 1–6). Groups 1–3 were added to the well plate directly; groups 4–6 were added to the fiber matrix, which was placed in centrifugal filters of 0.45 μM (Thermo Fisher). After adding water, mixing by pipetting, and centrifuging at 10 000 r·min^{-1} (Sigma 1-14 centrifuge) for 5 min, the activities of the samples were measured. Group 1: LDH only; group 2: LDH + sugars; group 3: LDH + sugars + BSA; group 4: LDH + sugars; group 5: mixture of LDH with sugars and BSA; group 6: after adding sugar solution with BSA, LDH with sugars was added. (b) Percent retained activities of dried LDH stabilized by MART-DA drying and MART-V drying. (c–e) SEM images of (c) preloaded fiber matrix, (d) fiber matrix after MART-DA drying with formulated LDH, and (e) fiber matrix after MART-V drying with formulated LDH. Measurements were conducted after drying and after one week of storage at 40 °C. Results are presented as mean ± sem; n = 3; $^{**}P < 0.01$.

Both methods preserved over 90% of the initial proteins. However, the protein quantification for 1 μg of LDH cannot be conducted before and after drying. The addition of BSA was aimed to minimize the loss of the desired protein due to non-specific binding. However, the protein measurement also detected the BSA, introducing potential inaccuracies in the results.

SEM was used to observe the morphology of the fiber matrix before and after MART drying, as shown in Figs. 3(c)–(e). The native state of the cellulose fiber matrix did not show any noticeable deposition between the fibers (Fig. 3(c)). However, after MART drying, sugar films were formed between the fibers (Figs. 3(d) and (e)), due to capillary bridges that formed between the fibers during the drying process. The Marangoni effect, which is caused by surface tension gradients, resulted in the gathering of proteins in the sugar films, where they were immobilized after drying. The formation of these sugar films was facilitated by the shape of the capillary bridge and the properties of trehalose [47]. The SEM analysis also showed that the MART-V drying technique produced a more elegant surface morphology compared with direct vacuum drying (Fig. S7 in Appendix A). When the formulated LDH solution was dried without the fiber matrix, it bubbled under a vacuum. However, when MART-V drying was used with the fiber matrix, the flat and smooth surface of the sugar films suggested that bubbling was inhibited.

Overall, the MART drying techniques showed promising results in the stabilization of a functional protein, LDH, on the cellulose fiber matrix. The MART drying technique offers several advantages over traditional lyophilization, including shorter drying period, lower energy consumption, and no refrigeration requirement. However, MART drying requires a considerably higher concentration of protective agents, particularly sugars, compared to freeze drying. In addition, supplementing the formulation with BSA can reduce the non-specific binding of the fiber matrix, and the selected cellulose fiber matrix should support the deposition of sugar films to immobilize and stabilize function proteins. The high retained activity of LDH after MART-V drying suggests that this technique may eliminate the risk of freeze damage to proteins, although this is largely dependent on the drying rate or the power of the vacuum pump. In contrast, MART-DA drying can completely avoid freezing stresses by keeping the wet-bulb temperature above 0 °C during the whole drying process.

3.2. MART drying of FGF-2

Fibroblast growth factors are a family of protein mitogens regulating cell proliferation, differentiation, and migration [50,84]. Among this family, FGF-2 or basic fibroblast growth factor is commonly found in wound fluids, especially at the earliest stage [85–89], where it stimulates the proliferation and differentiation of cells and their derivates [89–93]. It has been found that 100 $ng \cdot mL^{-1}$ of FGF-2 significantly increased the proliferation of mesenchymal stem cells [94,95]. However, FGF-2 must be stored in a frozen state, and the efficacy of FGF-2 can be substantially reduced under room temperature storage, limiting its applications [96,97].

In this study, 1 μg of FGF-2 was dried on fiber matrices with 1 M trehalose, 10% dextran, and 100 μg of BSA through each drying protocol: MART-V drying and MART-DA drying. Following one week of storage at 40 °C, the dried FGF-2 (1 μg) was reconstituted in 10 mL of culture medium. The efficacy of the reconstituted FGF-2 was investigated through its effect on the proliferation of MSC-hTERT. MSC-hTERT cells do not reduce growth and proliferation due to aging *in vitro* [98]. Since non-aseptic conditions were applied during drying, the reconstituted FGF-2 solutions were filtered with a 0.22 μM filter before being added to cells.

In addition, the results of the cell culture experiments demonstrated that the native fiber matrices were biocompatible with human mesenchymal stem cells, as evidenced by their morphology and proliferation (Fig. 4).

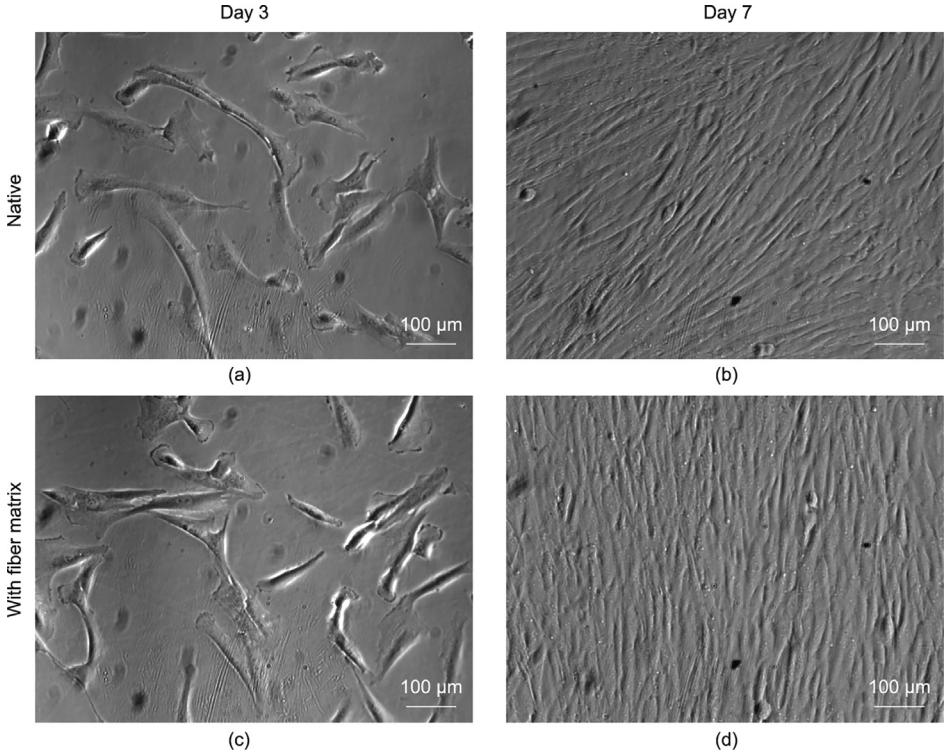


Fig. 4. Morphology of cells when cultured with the cellulose fiber matrix. (a, c) Cell morphology after culturing for 3 days (a) without the fiber matrix and (c) with the fiber matrix. (b, d) Cell morphology after culturing for 7 days (b) without the fiber matrix and (d) with the fiber matrix.

Regarding the proliferation with different culture mediums, cell numbers were normalized by the initial cell count. As demonstrated in Fig. 5(a), MSC-hTERT cells treated with FGF-2, whether they were exposed to MART-V-dried (group A), MART-DA-dried (group B), or fresh (group C) FGF-2, all exhibited substantially higher proliferation rates than the control groups, cells without FGF-2 (groups D and E). The cells treated with FGF-2 showed more than a four-fold increase in cell numbers, while the cells without FGF-2 showed only a three-fold increase. Moreover, both the MART-DA-dried and MART-V-dried FGF-2 exhibited no significant difference in improving the proliferation of MSC-hTERT cells and had a comparable cell-doubling level to that of fresh FGF-2 (Fig. 5(b)).

Hence, thermostabilized FGF-2 dried on a biocompatible fiber matrix through MART drying techniques could be used for wound healing and cosmetic applications, due to its extended shelf life and ease of shipping.

3.3. MART drying RT-LAMP reagents

RT-LAMP has been applied to rapid COVID-19 detection and other pathogens due to its simplicity and fast reaction time [53,54,99–103]. This technique does not require sample pretreatment, such as nucleic acid extraction, and the reaction can be finished within 30 min at one constant temperature of around 65 °C [104,105]. However, the enzymes, reverse transcriptase and Bst 2.0 polymerase, are thermolabile and required to be stored at –20 °C, which limits this technique's application in diagnostics and makes transportation difficult, especially in resource-limited areas. In this study, RT-LAMP reagents, including enzymes, deoxyribonucleoside triphosphates (dNTPs), labeled primers, and essential salts, were stabilized on a cellulose fiber matrix by MART-V drying, which extended the shelf life of the reagents to at least one week when stored at 40 °C.

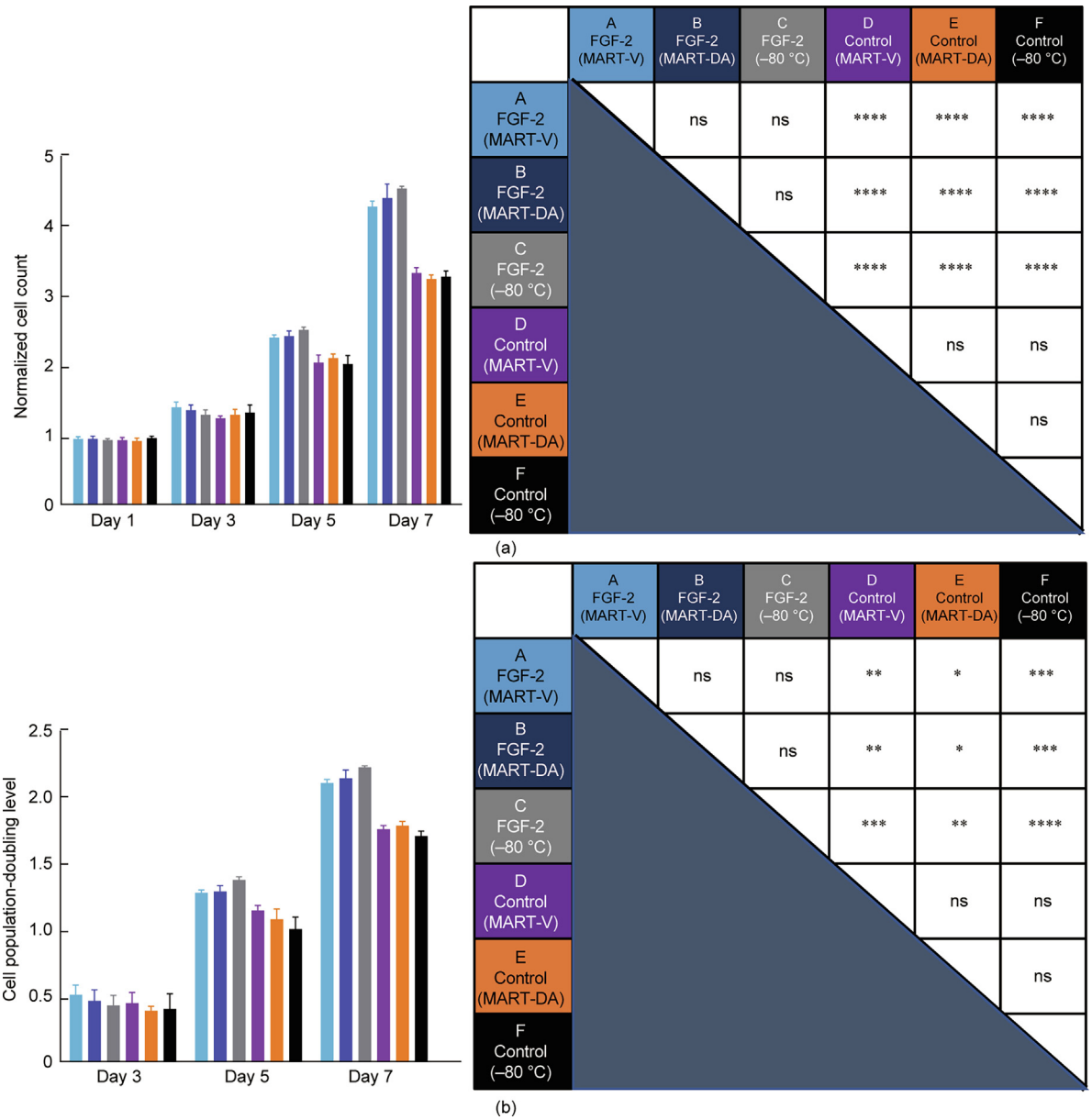


Fig. 5. Cell proliferation test with MART-dried FGF-2 after one week of storage at 40 °C. (a, b) CCK-8 assay on MSC-hTERT proliferation, presented as (a) normalized cell count and (b) cell population-doubling level. The table shows six different culture mediums, groups A–E, which were used to culture cells. Results in the bar chart are presented as mean ± sem; statistical relationships between groups are presented in the table next to the figure; $n = 3$; $^{*}P \leq 0.05$, $^{**}P \leq 0.01$, $^{***}P \leq 0.001$, and $^{****}P \leq 0.0001$.

Fluorescein FAM and biotin were attached to the FIP and BIP of the primers, respectively (Table S1). After amplification, the amplicons were labeled with both FAM and biotin. When the amplified products are added in, mixing with the phosphate buffer, FAM will bind with anti-FAM functionalized with gold nanoparticles (Au-NPs) in a conjugate pad. As the Au-NP-labeled amplicons move along the lateral flow stripe due to the capillary forces, they will be trapped by streptavidin pre-deposited at the test line. The test and control zone will be stained according to the amplicons. The results of the lateral flow test can be interpreted by the naked eye and will not be significantly affected by the pH of samples. The sensitivity of the lateral flow strips is demonstrated in Fig. S8 in Appendix A. These strips are capable of detecting LAMP amplicons, typically up to a 1000-fold dilution, with a concentration of around 0.5 $\mu g \cdot mL^{-1}$.

The previous size of the cellulose fiber matrix used for LDH and FGF-2 was fitted for lyophilization vials but was too large for PCR tubes. A reduced size of fiber matrix, at 5 mg, was implemented. The methodology of MART-V drying appeared to be a suitable method for stabilizing RT-LAMP reagents in comparison with MART-DA drying, due to its advantages in operation and manufacturing. More specifically, MART-V drying allows for the loading of fiber matrices into various containers, such as PCR tubes or *in vitro* devices prior to the addition of functional proteins. Subsequently, if a specialized freeze dryer is employed, PCR tubes can be automatically sealed to minimize the risk of contamination. In this case, only the vacuum pump of the freeze dryer is utilized without any freezing process. Conversely, with MART-DA drying, the fiber matrices containing RT-LAMP reagents are subjected to circulated dry air and must then be transferred to containers within a glove box with low relative humidity. Moreover, the stiffness of the dried fiber matrix may increase the difficulty of fitting into the tubes or devices with MART-DA drying.

RT-LAMP reagents were formulated and stabilized by means of MART-V drying (Fig. 6(a)). After 3 h of MART-V drying followed by one week of storage at 40 °C, the sensitivity of the MART-V-dried LAMP reagents was evaluated by means of a full-length RNA template (Twist Control 2). The MART-V-dried RT-LAMP reagents were able to detect sameples with a CT value of 33.7 (Fig. 6(b)). The corresponding qPCR assays for the same samples are presented in Fig. S8. The results of the lateral flow test were consistent with the results obtained from gel electrophoresis, as demonstrated in Fig. S9 in Appendix A.

RT-LAMP reagents, consisting of labeled primers and two functional proteins, were successfully thermostabilized by MART-V drying. After one week of storage at 40 °C, the dried reagents were able to detect samples with CT of 33.7. The thermostabilized RT-LAMP reagents can potentially be used for other types of pathogen detection by changing the primers. In addition, the success of the method in stabilizing multiple functional proteins on the fiber matrix could expand its potential applications.

3.4. Discussion

MART drying has proven effective in preserving the biofunctionalities of proteins and stabilizing them at ambient temperatures and even elevated temperatures. Notably, capillary bridges were observed within the biocompatible cellulose fiber matrix after both the MART-DA drying and MART-V drying protocols. While a small portion of proteins experienced adsorption on the solid surface, resulting in a loss of their potencies. This issue was effectively mitigated through BSA coating. The majority of the

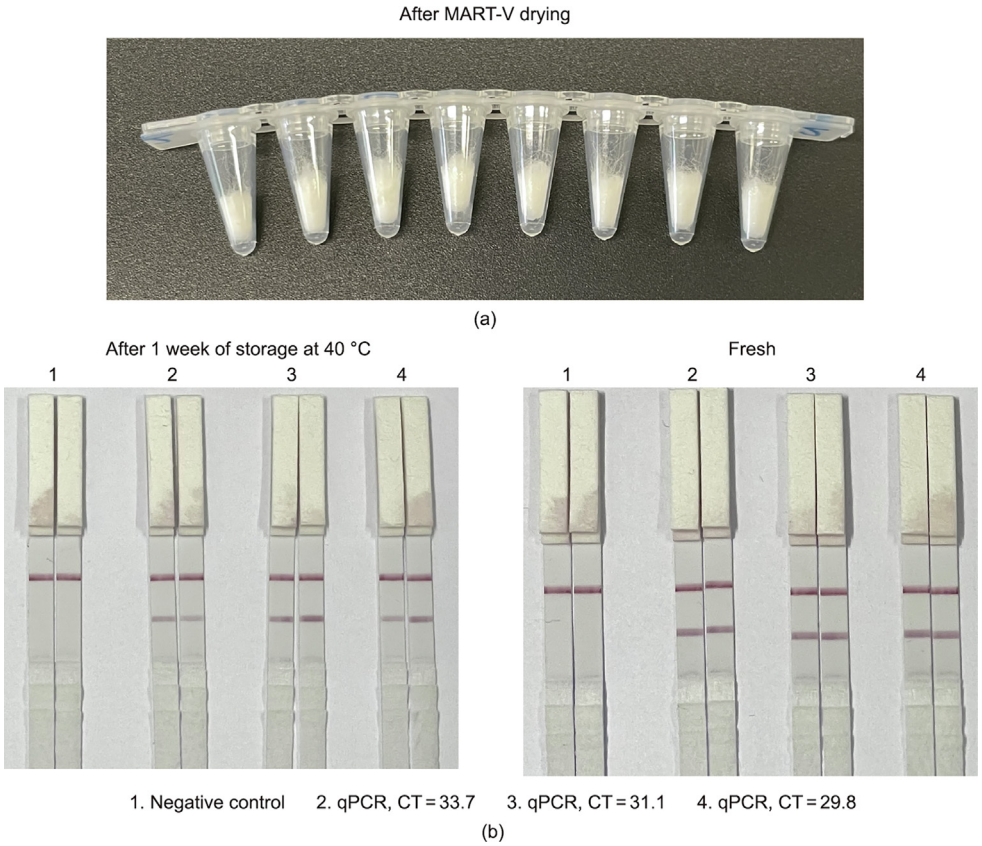


Fig. 6. MART-V drying of RT-LAMP reagents. (a) The fiber matrix with dried RT-LAMP reagents. (b) The LFT results after RT-LAMP reactions with samples 1–4 of different template concentrations. The same batch of samples 1–4 was evaluated by qPCR assays as well; the concentration of template is represented by CT values.

functional proteins were encapsulated within the capillary bridges formed by the protective agents, which offered 3D protection and improved the potencies after drying and storage. Moreover, freezing stresses could potentially be prevented, preserving the biofunctionalities of proteins during the drying process.

The outstanding advantages of MART drying are that it is simple, fast, and economical in terms of equipment and energy consumption. However, the formulation including the selection and concentrations of sugars and other excipients is the key to success. Although there is still a lack of definite prediction indicators of success, it is known that the capillary bridging formation is an essential condition. Hence small-scale testing on this aspect of the constituted bioproduct formulation can easily be carried out as a starting point.

Another advantage of MART drying is its ability to scale up. The proteins or other bioproducts can be stored within any containers or open trays, and the drying can be performed with industrial dryers, as long as aseptic conditions can be maintained. MART-V can speed up the drying process, but it is not essential.

A major limitation of this reported work is the lack of quantification of the coupled heat and mass transfer rates and their effect on the drying rate. The energy supplied to the drying samples ultimately affects the mass transfer (evaporation) rate and hence the drying time. In the experiments, the heat and mass transfer rates were not measured. The sample size was small and the surface-to-volume ratio was large. The assumption that heat transfer was not a limiting factor could be approximated under the conditions of the experiments. In scaled-up applications, heat transfer must be considered, and an additional and active energy supply could be provided to control or speed up the drying rates.

4. Conclusions

This study aimed to stabilize four functional proteins, namely LDH, FGF-2, and the mixture of reverse transcriptase and Bst 2.0 polymerase, on a cellulose fiber matrix through MART drying. The application of high concentrations of protective agents in this technique was found to effectively inhibit stress relaxation and preserve protein potency after drying and storage, despite some loss due to matrix surface adsorption. To reduce this non-specific binding on the fiber matrix, BSA coating was tested and found to be a viable solution.

Two different drying protocols, MART-DA and MART-V, were used to immobilize and stabilize functional proteins in sugar films, supported by a biocompatible fiber matrix. Both techniques provided comparable performance in functional protein stabilization, but each had its own advantages. MART-DA drying consumed less energy and involved only the use of dry air to remove moisture from the samples; however, it took 18 h to complete. This prolonged drying process could be improved by further coupling the heat and mass transfer analysis in the future work. Although MART-V drying significantly reduced the drying period, the energy consumption was increased due to the use of a vacuum pump.

In summary, MART drying is a simple and cost-effective drying strategy for long-term functional protein storage. In addition, the softness of the fiber matrix allows for its compression into any shape of container, further extending its possible applications.

CRediT authorship contribution statement

Yejiong Yu: Methodology, Formal analysis, Writing – original draft, Data curation, Investigation, Conceptualization. **Siqi Dai:** Writing – review & editing, Data curation, Formal analysis. **Johnny Xiangyi Zhou:** Writing – review & editing, Investigation, Formal analysis, Methodology, Data curation. **Wei E. Huang:** Writing – review & editing, Supervision, Methodology, Investigation, Conceptualization. **Zhanfeng Cui:** Resources, Project administration, Methodology, Investigation, Conceptualization, Writing – review & editing, Supervision.

Declaration of competing interest

Zhanfeng Cui is an Editorial Board Member for this journal and was not involved in the editorial review or the decision to publish this article. The authors declare that they have no known competing financial interests or personal relationships that could have appeared to influence the work reported in this paper.

Acknowledgments

Yejiong Yu expresses gratitude to Dr. Liyiwen Yuan for the help with SEM imagining.

Appendix A. Supplementary data

Supplementary data to this article can be found online at https://doi.org/10.1016/j.eng.2025.08.045.

References

[1] Modarres HP, Mofrad MR, Sanati-Nezhad A. Protein thermostability engineering. RSC Adv 2016;6(116):115252–70.
[2] Ghosh K, Dill K. Cellular proteomes have broad distributions of protein stability. Biophys J 2010;99(12):3996–4002.
[3] Brown LR. Commercial challenges of protein drug delivery. Expert Opin Drug Deliv 2005;2(1):29–42.
[4] Sykes C. Time- and temperature-controlled transport: supply chain challenges and solutions. Pharm Ther 2018;43(3):154–7,170.
[5] Frokjaer S, Otzen DE. Protein drug stability: a formulation challenge. Nat Rev Drug Discov 2005;4(4):298–306.
[6] Singh SK. Storage considerations as part of the formulation development program for biologics. Am Pharm Rev 2007;10(3):26–33.
[7] Webb SD, Webb JN, Hughes TG, Sesin DF, Kincaid AC. Freezing bulk-scale biopharmaceuticals using common techniques and the magnitude of freeze-concentration. BioPharm 2002;15(5):22–34.
[8] Singh SK, Kolhe P, Wang W, Nema S. Large-scale freezing of biologics: a practitioner's review, part 2: practical advice. Bioprocess Int 2009;7(10):34–42.
[9] Franks F. Freeze-drying of bioproducts: putting principles into practice. Eur J Pharm Biopharm 1998;45(3):221–9.
[10] Liu J, Viverette T, Virgin M, Anderson M, Dalal P. A study of the impact of freezing on the lyophilization of a concentrated formulation with a high fill depth. Pharm Dev Technol 2005;10(2):261–72.
[11] Dixon D, Tchessalov S, Barry A, Warne N. The impact of protein concentration on mannitol and sodium chloride crystallinity and polymorphism upon lyophilization. J Pharm Sci 2009;98(9):3419–29.
[12] Thorat AA, Suryanarayanan R. Characterization of phosphate buffered saline (PBS) in frozen state and after freeze-drying. Pharm Res 2019;36(7):98.
[13] Shalaev E. The impact of buffer on processing and stability of freeze-dried dosage forms. I. Solution freezing behavior. Am Pharm Rev 2005;8(5):80–7.
[14] Arsiccio A, Pisano R. The ice–water interface and protein stability: a review. J Pharm Sci 2020;109(7):2116–30.
[15] Kolhe P, Holding E, Lary A, Chico S, Singh SK. Large-scale freezing of biologics: understanding protein and solute concentration changes in a cryovessel—part 2. BioPharm Int 2010;23(7):40–9.
[16] Thielmann A, Viehmann A, Weltermann BM. Effectiveness of a web-based education program to improve vaccine storage conditions in primary care (keep cool): study protocol for a randomized controlled trial. Trials 2015;16(1):301.
[17] Chesko J, Fox C, Dutill T, Vedvick T, Reed S. Lyophilization and stabilization of vaccines. In: Singh M, Srivastava IK, editors. Development of vaccines: from discovery to clinical testing. Hoboken: John Wiley & Sons, Inc.; 2011. p. 385–97.
[18] Kartoglu U, Milstien J. Tools and approaches to ensure quality of vaccines throughout the cold chain. Expert Rev Vaccines 2014;13(7):843–54.
[19] Kumru OS, Joshi SB, Smith DE, Middaugh CR, Prusik T, Volkin DB. Vaccine instability in the cold chain: mechanisms, analysis and formulation strategies. Biologicals 2014;42(5):237–59.
[20] Larena Fernández I, Vara Callau M, Peña Blasco G, Atance Melendo E, Gay Gasanz B, Blasco Pérez-Aramendía MJ. Vaccine cold chain interruption in a primary care centre and economic evaluation. Enferm Clín Engl Ed 2017;27(1):44–8.

[21] Wolfson LJ, Gasse F, Lee-Martin SP, Lydon P, Magan A, Tibouti A, et al. Estimating the costs of achieving the WHO–UNICEF Global Immunization Vision and Strategy, 2006–2015. Bull World Health Organ 2008;86(1):27–39.
[22] Cheyne J. Vaccine delivery management. Rev Infect Dis 1989;11(Suppl 3): S617–22.
[23] Bishai DM, Bhatt S, Miller LT, Hayden GF. Vaccine storage practices in pediatric offices. Pediatrics 1992;89(2):193–6.
[24] Zhang J, Pritchard E, Hu X, Valentin T, Panilaitis B, Omenetto FG, et al. Stabilization of vaccines and antibiotics in silk and eliminating the cold chain. Proc Natl Acad Sci USA 2012;109(30):11981–6. Retraction in: Zhang J, Pritchard E, Hu X, Valentin T, Panilaitis B, Omenetto FG, et al. Proc Natl Acad Sci USA 2016;113(26):E3810.
[25] Rathore N, Rajan RS. Current perspectives on stability of protein drug products during formulation, fill and finish operations. Biotechnol Prog 2008;24(3):504–14.
[26] Jain NK, Sahni N, Kumru OS, Joshi SB, Volkin DB, Russell MC. Formulation and stabilization of recombinant protein based virus-like particle vaccines. Adv Drug Deliv Rev 2015;93:42–55.
[27] Balcão VM, Vila MMDC. Structural and functional stabilization of protein entities: state-of-the-art. Adv Drug Deliv Rev 2015;93:25–41.
[28] Cicerone MT, Pikal MJ, Qian KK. Stabilization of proteins in solid form. Adv Drug Deliv Rev 2015;93:14–24.
[29] Emami F, Vatanara A, Park EJ, Na DH. Drying technologies for the stability and bioavailability of biopharmaceuticals. Pharmaceutics 2018;10(3):131.
[30] Grasmeijer N, Tiraboschi V, Woerdenbag HJ, Frijlink HW, Hinrichs WLJ. Identifying critical process steps to protein stability during spray drying using a vibrating mesh or a two-fluid nozzle. Eur J Pharm Sci 2019;128:152–7.
[31] Roy I, Gupta MN. Freeze-drying of proteins: some emerging concerns. Biotechnol Appl Biochem 2004;39(2):165–77.
[32] Merivaara A, Zini J, Koivunotko E, Valkonen S, Korhonen O, Fernandes FM, et al. Preservation of biomaterials and cells by freeze-drying: change of paradigm. J Control Release 2021;336:480–98.
[33] Hansen LJJ, Daoussi R, Vervaet C, Remon JP, De Beer TRM. Freeze-drying of live virus vaccines: a review. Vaccine 2015;33(42):5507–19.
[34] Luthra S, Obert JP, Kalonia DS, Pikal MJ. Investigation of drying stresses on proteins during lyophilization: differentiation between primary and secondary-drying stresses on lactate dehydrogenase using a humidity controlled mini freeze-dryer. J Pharm Sci 2007;96(1):61–70.
[35] Liu J. Physical characterization of pharmaceutical formulations in frozen and freeze-dried solid states: techniques and applications in freeze-drying development. Pharm Dev Technol 2006;11(1):3–28.
[36] Telikepalli S, Kumru OS, Kim JH, Joshi SB, O'Berry KB, Blake-Haskins AW, et al. Characterization of the physical stability of a lyophilized IgG1 mAb after accelerated shipping-like stress. J Pharm Sci 2015;104(2):495–507.
[37] Stratta L, Capozzi LC, Franzino S, Pisano R. Economic analysis of a freeze-drying cycle. Processes 2020;8(11):1399.
[38] Sun D, Cao C, Li B, Chen H, Cao P, Li J, et al. Study on combined heat pump drying with freeze-drying of Antarctic krill and its effects on the lipids. J Food Process Eng 2017;40(6):e12577.
[39] Yu Y. Matrix assisted room temperature and vacuum drying of functional proteins and applications [dissertation]. Oxford: University of Oxford; 2021.
[40] Alcock R, Cottingham MG, Rollier CS, Furze J, De Costa SD, Hanlon M, et al. Long-term thermostabilization of live poxviral and adenoviral vaccine vectors at supraphysiological temperatures in carbohydrate glass. Sci Transl Med 2010;2(19):19ra12.
[41] Davidson T. Vaccines: history, science, and issues (the story of a drug). Santa Barbara: ABC-Clio/Greenwood; 2017.
[42] Leung V, Szewczyk A, Chau J, Hosseinidoust Z, Groves L, Hawsawi H, et al. Long-term preservation of bacteriophage antimicrobials using sugar glasses. ACS Biomater Sci Eng 2018;4(11):3802–8.
[43] Dulal P, Wright D, Ashfield R, Hill AVS, Charleston B, Warimwe GM. Potency of a thermostabilised chimpanzee adenovirus Rift Valley Fever vaccine in cattle. Vaccine 2016;34(20):2296–8.
[44] Leung V, Mapletoft J, Zhang A, Lee A, Vahedi F, Chew M, et al. Thermal stabilization of viral vaccines in low-cost sugar films. Sci Rep 2019;9:7631.
[45] Minamoto K, Nagano M, Inaoka T, Kitano T, Ushijima K, Fukuda Y, et al. Skin problems among fiber-glass reinforced plastics factory workers in Japan. Ind Health 2002;40(1):42–50.
[46] Dulal P. Investigation of sugar-membrane vaccine stabilisation for improved vaccine thermostability and delivery [dissertation]. Oxford: University of Oxford; 2016.
[47] Yu Y, Yang A, Ye H, Dye JF, Cui Z. Numerical study of the formation and drying kinetics of a capillary bridge of trehalose solution between two parallel hydrophilic fibres. Chem Eng Sci 2020;226:115849.
[48] Pikal-Cleland KA, Rodríguez-Hornedo N, Amidon GL, Carpenter JF. Protein denaturation during freezing and thawing in phosphate buffer systems: monomeric and tetrameric β-galactosidase. Arch Biochem Biophys 2000;384 (2):398–406.
[49] Park H, Park JY, Park KM, Chang PS. Effects of freezing rate on structural changes in *L*-lactate dehydrogenase during the freezing process. Sci Rep 2021;11:13643.
[50] Kottakis F, Polytarchou C, Foltopoulou P, Sanidas I, Kampranis SC, Tsichlis PN. FGF-2 regulates cell proliferation, migration, and angiogenesis through an NDY1/KDM2B–miR-101–EZH2 pathway. Mol Cell 2011;43(2):285–98.
[51] Kotani E, Yamamoto N, Kobayashi I, Uchino K, Muto S, Ijiri H, et al. Cell proliferation by silk gut incorporating FGF-2 protein microcrystals. Sci Rep 2015;5:11051.
[52] Yu HC, Huang FM, Lee SS, Yu CC, Chang YC. Effects of fibroblast growth factor-2 on cell proliferation of cementoblasts. J Dent Sci 2016;11(4):463–7.
[53] Lim B, Ratcliff J, Nawrot DA, Yu Y, Sanghani HR, Hsu CC, et al. Clinical validation of optimised RT-LAMP for the diagnosis of SARS-CoV-2 infection. Sci Rep 2021;11:16193.
[54] Huang WE, Lim B, Hsu CC, Xiong D, Wu W, Yu Y, et al. RT-LAMP for rapid diagnosis of coronavirus SARS-CoV-2. J Microbial Biotechnol 2020; 13(4):950–61.
[55] Bhatnagar BS, Bogner RH, Pikal MJ. Protein stability during freezing: separation of stresses and mechanisms of protein stabilization. Pharm Dev Technol 2007;12(5):505–23.
[56] Cao E, Chen Y, Cui Z, Foster PR. Effect of freezing and thawing rates on denaturation of proteins in aqueous solutions. Biotechnol Bioeng 2003;82 (6):684–90.
[57] Starnes JW. Effect of storage conditions on lactate dehydrogenase released from perfused hearts. Int J Cardiol 2008;127(1):114–6.
[58] Carpenter JF, Prestrelski SJ, Arakawa T. Separation of freezing- and drying-induced denaturation of lyophilized proteins using stress-specific stabilization: I. enzyme activity and calorimetric studies. Arch Biochem Biophys 1993;303(2):456–64.
[59] Al-Hussein A, Gieseler H. Investigation of histidine stabilizing effects on LDH during freeze-drying. J Pharm Sci 2013;102(3):813–26.
[60] Manning MC, Chou DK, Murphy BM, Payne RW, Katayama DS. Stability of protein pharmaceuticals: an update. Pharm Res 2010;27(4):544–75.
[61] Nakanishi K, Sakiyama T, Imamura K. On the adsorption of proteins on solid surfaces, a common but very complicated phenomenon. J Biosci Bioeng 2001;91(3):233–44.
[62] Abdel-Rahman EA, Smejkal Q, Schick R, El-Syiad S, Kurz T. Influence of dextran concentrations and molecular fractions on the rate of sucrose crystallization in pure sucrose solutions. J Food Eng 2008;84(4):501–8.
[63] Le Meste M, Champion D, Roudaut G, Blond G, Simatos D. Glass transition and food technology: a critical appraisal. J Food Sci 2002;67(7):2444–58.
[64] Liu Y, Bhandari B, Zhou W. Glass transition and enthalpy relaxation of amorphous food saccharides: a review. J Agric Food Chem 2006;54 (16):5701–17.
[65] Yu L. Amorphous pharmaceutical solids: preparation, characterization and stabilization. Adv Drug Deliv Rev 2001;48(1):27–42.
[66] Brawer SA. Theory of relaxation in viscous liquids and glasses. J Chem Phys 1984;81(2):954–75.
[67] Surana R, Pyne A, Rani M, Suryanarayanan R. Measurement of enthalpic relaxation by differential scanning calorimetry—effect of experimental conditions. Thermochim Acta 2005;433(1–2):173–82.
[68] Putri NI, Van Audenhove J, Kyomugasho C, Van Loey A, Hendrickx M. Relaxation temperature and storage stability of the functionalized cell wall material residue from lemon peel. Food Hydrocoll 2024;150:109711.
[69] Frauenfelder H, Chen G, Berendzen J, Fenimore PW, Jansson H, McMahon BH, et al. A unified model of protein dynamics. Proc Natl Acad Sci USA 2009;106 (13):5129–34.
[70] Kissi EO, Grohganz H, Löbmann K, Ruggiero MT, Zeitler JA, Rades T. Glass-transition temperature of the β-relaxation as the major predictive parameter for recrystallization of neat amorphous drugs. J Phys Chem B 2018;122 (10):2803–8.
[71] Lai MC, Topp EM. Solid-state chemical stability of proteins and peptides. J Pharm Sci 1999;88(5):489–500.
[72] Vallaster B, Engelsing F, Grohganz H. Influence of water and trehalose on α- and β-relaxation of freeze-dried lysozyme formulations. Eur J Pharm Biopharm 2024;194:1–8.
[73] Starciuc T, Malfait B, Danede F, Paccou L, Guinet Y, Correia NT, et al. Trehalose or sucrose: which of the two should be used for stabilizing proteins in the solid state? A dilemma investigated by *in situ* micro-Raman and dielectric relaxation spectroscopies during and after freeze-drying. J Pharm Sci 2020;109(1):496–504.
[74] Schersch K, Betz O, Garidel P, Muehlau S, Bassarab S, Winter G. Systematic investigation of the effect of lyophilizate collapse on pharmaceutically relevant proteins I: stability after freeze-drying. J Pharm Sci 2010;99 (5):2256–78.
[75] Schwegman JJ, Hardwick LM, Akers MJ. Practical formulation and process development of freeze-dried products. Pharm Dev Technol 2005;10 (2):151–73.
[76] Ma GJ, Ferhan AR, Jackman JA, Cho NJ. Conformational flexibility of fatty acid-free bovine serum albumin proteins enables superior antifouling coatings. Commun Mater 2020;1:45.
[77] Banerjee I, Pangule RC, Kane RS. Antifouling coatings: recent developments in the design of surfaces that prevent fouling by proteins, bacteria, and marine organisms. Adv Mater 2011;23(6):690–718.
[78] Wang LS, Gupta A, Duncan B, Ramanathan R, Yazdani M, Rotello VM. Biocidal and antifouling chlorinated protein films. ACS Biomater Sci Eng 2016;2 (11):1862–6.
[79] Lin Y, Liu K, Wang C, Li L, Liu Y. Electrochemical immunosensor for detection of epidermal growth factor reaching lower detection limit: toward oxidized glutathione as a more efficient blocking reagent for the antibody functionalized silver nanoparticles and antigen interaction. Anal Chem 2015;87(16):8047–51.
[80] Cai B, Hu K, Li C, Jin J, Hu Y. Bovine serum albumin bioconjugated graphene oxide: red blood cell adhesion and hemolysis studied by QCM-D. Appl Surf Sci 2015;356:844–51.

[81] Steinitz M. Quantitation of the blocking effect of Tween 20 and bovine serum albumin in ELISA microwells. Anal Biochem 2000;282(2):232–8.
[82] Besecker J, Cornell KA, Hampikian G. Dynamic passivation with BSA overcomes LTCC mediated inhibition of PCR. Sens Actuators B 2013;176:118–23.
[83] Wang LS, Gopalakrishnan S, Luther DC, Rotello VM. Protein-based films as antifouling and drug-eluting antimicrobial coatings for medical implants. ACS Appl Mater Interfaces 2021;13(40):48301–7.
[84] Rubert Pérez CM, Álvarez Z, Chen F, Aytun T, Stupp SI. Mimicking the bioactivity of fibroblast growth factor-2 using supramolecular nanoribbons. ACS Biomater Sci Eng 2017;3(9):2166–75.
[85] Cooper ML, Spielvogel RL. Artificial skin for wound healing. Clin Dermatol 1994;12(1):183–91.
[86] Chen WYJ, Rogers AA, Lydon MJ. Characterization of biologic properties of wound fluid collected during early stages of wound healing. J Invest Dermatol 1992;99(5):550–8.
[87] Gu TM, Niu XT, Guo H. Clinical observation on changes of fibroblast growth factor in burn wounds. Chin J Repar Reconstr Surg 2000;14(5):261–3. Chinese.
[88] Vogt PM, Lehnhardt M, Wagner D, Jansen V, Krieg M, Steinau HU. Determination of endogenous growth factors in human wound fluid: temporal presence and profiles of secretion. Plast Reconstr Surg 1998;102 (1):117–23.
[89] Ching YH, Sutton TL, Pierpont YN, Robson MC, Payne WG. The use of growth factors and other humoral agents to accelerate and enhance burn wound healing. Eplasty 2011;11:e41.
[90] Akita S, Akino K, Imaizumi T, Hirano A. Basic fibroblast growth factor accelerates and improves second-degree burn wound healing. Wound Repair Regen 2008;16(5):635–41.
[91] Montesano R, Vassalli JD, Baird A, Guillemin R, Orci L. Basic fibroblast growth factor induces angiogenesis *in vitro*. Proc Natl Acad Sci USA 1986;83 (19):7297–301.
[92] Steed DL. The role of growth factors in wound healing. Surg Clin North Am 1997;77(3):575–86.
[93] Nissen NN, Polverini PJ, Gamelli RL, DiPietro LA. Basic fibroblast growth factor mediates angiogenic activity in early surgical wounds. Surgery 1996;119 (4):457–65.
[94] Stewart AA, Byron CR, Pondenis H, Stewart MC. Effect of fibroblast growth factor-2 on equine mesenchymal stem cell monolayer expansion and chondrogenesis. Am J Vet Res 2007;68(9):941–5.
[95] Fujimoto Y, Yokozeki T, Yokoyama A, Tabata Y. Basic fibroblast growth factor enhances proliferation and hepatocyte growth factor expression of feline mesenchymal stem cells. Regen Ther 2020;15:10–7.
[96] Shah DR. Effect of various additives on the stability of basic fibroblast growth factor and development of an intradermal injectable formulation [dissertation]. Kansas City: University of Missouri–Kansas City; 1998.
[97] Benington L, Rajan G, Locher C, Lim LY. Fibroblast growth factor 2—a review of stabilisation approaches for clinical applications. Pharmaceutics 2020;12 (6):508.
[98] An K, Liu H, Zhong X, Deng DYB, Zhang J, Liu Z. hTERT-immortalized bone mesenchymal stromal cells expressing rat galanin via a single tetracycline-inducible lentivirus system. Stem Cells Int 2017;2017:6082684.
[99] Thompson D, Lei Y. Mini review: recent progress in RT-LAMP enabled COVID-19 detection. Sens Actuators Rep 2020;2(1):100017.
[100] Yang W, Dang X, Wang Q, Xu M, Zhao Q, Zhou Y, et al. Rapid detection of SARS-CoV-2 using reverse transcription RT-LAMP method. 2020. medRxiv: 2020.03.02.20030130.
[101] Huang X, Tang G, Ismail N, Wang X. Developing RT-LAMP assays for rapid diagnosis of SARS-CoV-2 in saliva. eBioMedicine 2022;75:103736.
[102] Yu Y, Zhou JXY, Li B, Ji M, Wang Y, Carnaby E, et al. A quantitative RT-qLAMP for the detection of SARS-CoV-2 and human gene in clinical application. J Microbial Biotechnol 2022;15(10):2619–30.
[103] Cui Z, Chang H, Wang H, Lim B, Hsu CC, Yu Y, et al. Development of a rapid test kit for SARS-CoV-2: an example of product design. Biodes Manuf 2020;3 (2):83–6.
[104] Marino FE, Proffitt E, Joseph E, Manoharan A. A rapid, specific, extraction-less, and cost-effective RT-LAMP test for the detection of SARS-CoV-2 in clinical specimens. PLoS One 2022;17(4):e0266703.
[105] Dao Thi VL, Herbst K, Boerner K, Meurer M, Kremer LPM, Kirrmaier D, et al. A colorimetric RT-LAMP assay and LAMP-sequencing for detecting SARS-CoV-2 RNA in clinical samples. Sci Transl Med 2020;12(556):eabc7075.